New molecular catalysts for ATP cleavage. Criteria of size complementarity

Juan A. Aguilar,[a] Ana B. Descalzo,[b] Pilar Díaz,[b] Vieri Fusi,[c] Enrique García-España,[b] Santiago V. Luis,[d] Mauro Micheloni,[c] José A. Ramírez,[b] Paolo Romani[c] and Conxa Soriano[a]

[a] *Departamento de Química Orgánica, Facultad de Farmacia, Universidad de Valencia, 46100 Burjassot (Valencia), Spain*
[b] *Departamento de Química Inorgánica, Facultad de Química, Universidad de Valencia, C/ Dr. Moliner 50, 46100 Burjassot (Valencia), Spain. E-mail: enrique.garcia-es@uv.es*
[c] *Instituto di Scienze Chimiche, Università di Urbino, P.za Rinascimento 6, I-61209 Urbino, Italia*
[d] *Departamento de Química Orgánica e Inorgánica, Universidad Jaume I, 12080 Castellón, Spain*

Received (in Cambridge, UK) 21st January 2000, Accepted 17th March 2000
Published on the Web 9th May 2000

The interaction of the cyclophane receptor 2,5,8,11,14,17-hexaaza[18]metacyclophane (**L**) with the nucleotides ATP, ADP and AMP is described. **L** yields one of the largest rate enhancements for hydrolytic ATP cleavage observed in macrocyclic polyamines. The process is specific for the formation of ADP and involves a high degree of geometrical complementarity between host and guest species. The analogue compound 24-hydroxy-2,5,8,11,14,17-hexaaza[18]-metacyclophane (**L**^{1}) shows also a high degree of ATP activation. However, in this case deprotonation of the hydroxy group results in almost complete quenching of the ATPase activity above pH 7.0.

Introduction

Molecular catalysis is, together with molecular recognition, self-assembling and translocation, one of the corner-stones of supramolecular chemistry.[1] Therefore, many efforts have been devoted in the last few years to the design of molecular catalysts with ever increasing efficiency and specificity. In this sense, one of the processes that has given rise to a lot of interest is the catalytic cleavage of ATP to give ADP and inorganic phosphate, due to its ubiquitous participation in the bioenergetics of all living organisms. Different polyammonium compounds increase the rate of ATP cleavage.[1–5] Of these, two polyaza macrocycles have shown, by far, the largest rate enhancements. These compounds are the well-known 1,13-dioxa-4,7,10,16,19,22-hexaazacyclotetracosane (**O-bisdien**) which was first prepared and extensively studied by Lehn's and Mertes' groups[2] and the all aza macrocycle 1,4,7,10,13,16,19-heptaazacyclohenicosane (hereafter **[21]aneN$_7$**, see Chart 1).[3] All the other polyamines, either of cyclic or open-chain nature, present a much lower efficiency. Apart from pH, other factors affect the ability of the polyammonium receptors to induce rate accelerations of the ATP cleavage:[1–5] i) formation of stable anion complexes between host and guest species, ii) presence of nucleophilic nitrogens in the host species, iii) overall charge of the host–guest couple, iv) size complementarity, *etc*.

Here we report on a new cyclophane receptor 2,5,8,11,14,17-hexaaza[18]metacyclophane (**L**) (Chart 1) that shows a multipoint binding scheme with the nucleotides (hydrogen-bonding, electrostatic forces, π-stacking) and can be included in this first group of catalysts with **O-bisdien** and **[21]aneN$_7$**, displaying also a high degree of specificity for the conversion of ATP into ADP. The analysis of the catalytic results for this molecule and some analogues confirms the key role played by host–guest molecular and size complementarity in ATPase mimicking. This is further confirmed by the analogous receptor **L**^{1}, in which the benzene spacer has been replaced by a phenolic one. Indeed, deprotonation of the OH group of **L**^{1}, produces a

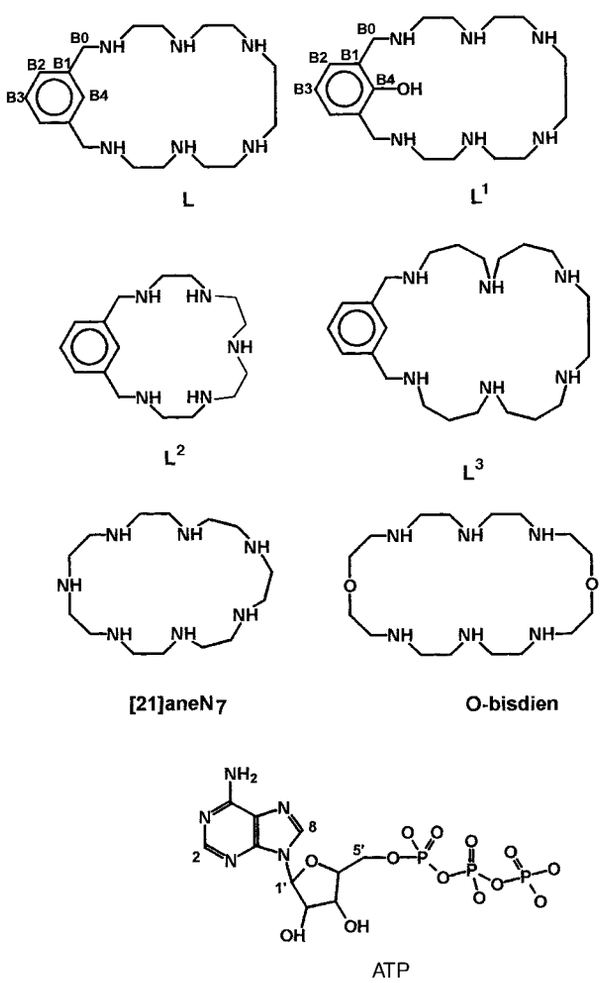

Chart 1

DOI: 10.1039/b000606h

destabilisation of the adduct species and an important size reduction of the macrocyclic cavity resulting in almost complete quenching of the catalytic activity.

Experimental

Synthesis of the receptors

2,5,8,11,14,17-Hexakis(*p*-tolylsulfonyl)-2,5,8,11,14,17-hexaaza[18]metacyclophane. The general procedure followed was that described in references 6 and 7 for related paracyclophanes. 1,4,7,10,13,16-Hexakis(*p*-tolylsulfonyl)-1,4,7,10,13,16-hexaazahexadecane (7 g, 6 mmol)[8] and an excess of K_2CO_3 (5.4 g, 39 mmol) were suspended in refluxing CH_3CN (250 cm^3). To this mixture 1,3-bis(bromomethyl)benzene (3.2 g, 12 mmol) in 250 cm^3 of CH_3CN was added dropwise over 6 hours. The suspension was refluxed for a further 48 h and then filtered. The solution was evaporated to dryness. The solid product was chromatographed on silica using ethyl acetate–hexane 2:1 mixture as eluent (1.5 g, 20%), mp 108–110 °C. δ_H ($CDCl_3$): 2.37 (s, 9H), 2.43 (s, 9H), 3.10–3.35 (m, 20H), 4.26 (s, 4H), 6.98–7.02 (m, 2H), 7.25–7.37 (m, 12H), 7.61–7.81 (m, 14H). δ_C ($CDCl_3$): 21.7, 48.4, 49.9, 50.0, 50.4, 50.6, 53.3, 127.1, 127.6, 127.7, 127.8, 129.0, 130.1, 134.7, 134.9, 136.0, 137.3, 143.8, 144.1. MS *m*/*z* (FAB) 1258 $(M + H)^+$.

2,5,8,11,14,17-Hexaaza[18]metacyclophane (L). On a suspension of 2,5,8,11,14,17-hexakis(*p*-tolylsulfonyl)-2,5,8,11,14,17-hexaaza[18]metacyclophane (1.5 g, 1.2 mmol) in diethyl ether (30 cm^3), and methanol (1 cm^3) cooled at −70 °C, ammonia (300 cm^3) was condensed. Small pieces of lithium were added to the mixture until the suspension became blue. After the solution remained blue for 30 min, NH_4Cl (6 g, 0.1 mol) was added. The white solid obtained after the evaporation of the solvents was treated with 3 mol dm^{-3} HCl (200 cm^3) and the resulting solution washed with $CHCl_3$ (3 × 100 cm^3). The acidic solution was filtered, and then evaporated to dryness. The resultant solid was dissolved in the minimum amount of water and the solution made alkaline with concentrated NaOH. The liquid was extracted with $CHCl_3$ (6 × 100 cm^3). The organic part was dried over Na_2SO_4 and vacuum evaporated to obtain a solid that was dissolved in ethanol and treated with 37% HCl until complete precipitation of a white solid that was filtered off to achieve **L** as its hexahydrochloride salt. Yield, 68%. δ_H (D_2O): 3.07 (s, 4H), 3.19 (m, 4H), 3.32 (m, 4H), 3.40 (m, 8H), 4.26 (s, 4H), 7.49 (s, 3H), 7.51 (s, 1H). δ_C (D_2O): 42.6, 43.6, 44.0, 44.5, 46.0, 51.2, 130.7, 131.4, 132.0, 132.4. Anal. Calcd for $C_{18}H_{40}Cl_6N_6$: C, 39.08; H, 7.29; N, 15.19. Found: C, 39.0; H, 7.4; N, 15.1%.

2,5,8,11,14,17-Hexakis(*p*-tolylsulfonyl)-24-hydroxy-2,5,8,11,14,17-hexaaza[18]metacyclophane. To prepare this compound the same experimental procedure followed for **L** and also described in refs. 6, 7 and 9 was followed, reacting 1,4,7,10,13,16-hexakis(*p*-tolylsulfonyl)-1,4,7,10,13,16-hexaazahexadecane and 2,6-bis(bromomethyl)anisole[9] in CH_3CN. Yield, 34%. δ_H ($CDCl_3$, 25 °C): 2.22 (s, 18H), 2.52 (m, 16H), 2.68 (s, 4H), 3.78 (s, 3H), 4.25 (s, 4H), 7.24 (t, 1H), 7.28 (d, 4H), 7.34 (d, 8H), 7.75 (d, 8H), 7.88 (d, 4H), 7.96 (d, 2H). δ_C ($CDCl_3$): 21.6, 47.3, 47.4, 49.4, 49.6, 50.5, 50.9, 62.1, 124.5, 127.7, 128.4, 130.2, 130.9, 134.5, 134.8, 135.9, 143.6, 143.7, 143.9, 158.7. MS *m*/*z* (FAB) 1291 $(M + H)^+$. Anal. Calcd for $C_{61}H_{72}N_6O_{13}S_6$: C, 56.81; H, 5.63; N, 6.52. Found: C, 56.9; H, 5.7; N, 6.5%.

24-Hydroxy-2,5,8,11,14,17-hexaaza[18]metacyclophane. The same procedure was used as for **L**. The reducing conditions of the treatment led also to the demethylation reaction of the ethereal methyl group of anisole, obtaining, after the usual work-up, ligand $\mathbf{L^1}$ that was purified as its hexahydrochloride salt. Yield 71%. δ_H (D_2O): 3.08 (s, 4H), 3.18 (m, 4H), 3.23 (m, 4H), 3.40 (m, 8H), 4.36 (s, 4H), 7.11 (t, 1H), 7.46 (d, 2H). δ_C (D_2O): 44.4, 45.3, 46.3, 47.3, 47.4, 48.2, 121.4, 123.9, 135.5, 155.4. Anal. Calcd for $C_{18}H_{40}Cl_6N_6O$: C, 37.98; H, 7.08; N, 14.76. Found: C, 37.9; H, 7.1; N, 14.7%.

Emf measurements

The potentiometric titrations were carried out at 298.1 ± 0.1 K in $NaClO_4$ 0.15 mol dm^{-3}. The experimental procedure used (burette, potentiometer, cell, stirrer, microcomputer, *etc*.) was the same as has been fully described elsewhere.[10] The acquisition of the emf data was performed with the computer program PASAT.[11] The reference electrode was an Ag/AgCl electrode in saturated KCl solution. The glass electrode was calibrated as an hydrogen-ion concentration probe by titration of previously standardised amounts of HCl with CO_2-free NaOH solutions and determining the equivalence point by the Gran's method,[12] which gives the standard potential, $E^{\circ\prime}$, and the ionic product of water ($pK_w = 13.73(1)$).

The computer program HYPERQUAD,[13] was used to calculate the protonation and stability constants. The titration curves for the systems ATP–**L** and ATP–$\mathbf{L^1}$ were both made from alkaline to acidic pH. In the evaluation of the constants just those points over pH *ca*. 3 were used, in order to avoid the rapid ATP cleavage that occurs at lower pH values. The titration curves for each system consisted of *ca.* 100 experimental points corresponding to at least two measurements and the concentration of ATP, ADP and of **L** and $\mathbf{L^1}$ ranged from 1×10^{-3} to 5×10^{-3} mol dm^{-3}. Protonation constants of ATP, ADP and AMP have been taken from ref. 3.

The different titration curves for each system were treated either as a single set or as separate curves without significant variations in the values of the stability constants. Finally, the sets of data were merged together and treated simultaneously to give the final stability constants.

NMR measurements

The ^{31}P NMR spectra were recorded at 121.42 MHz on a Varian Unity 300 MHz. Chemical shifts are relative to an external reference of 85% H_3PO_4. Adjustments to the desired pH were made using drops of HCl or NaOH solutions. Kinetic studies were performed by following at different pH values the time-dependent change in the integrals of the resolved ^{31}P NMR signals of P_α, P_β and P_γ of ATP and peaks for inorganic phosphate and ADP. The kinetic parameters for the conversion of ATP into ADP were calculated by following the disappearance with time of the P_β NMR signal in samples with molar ratio ATP : macrocycle ≤ 1 or the signal corresponding to formation of inorganic phosphate in samples with an excess of ATP. Initial concentrations of ATP and polyamines varied in the range 10^{-2}–3×10^{-2} mol dm^{-3}. Plots of log [ATP] *vs.* time were linear for several half-lives. The ^1H and ^{13}C NMR spectra were recorded on Varian UNITY 300 and UNITY 400 spectrometers, operating at 299.95 and 399.95 MHz for ^1H and at 75.43 and 100.58 MHz for ^{13}C. The spectra were obtained at room temperature in D_2O or $CDCl_3$ solutions. For the ^{13}C NMR spectra dioxane was used as a reference standard (δ = 67.4 ppm) and for the ^1H spectra the solvent signal was used. Adjustments to the desired pH were made using drops of HCl or NaOH solutions. The pH was calculated from the measured pD values using the correlation, pH = pD − 0.4.[14]

Spectrophotometric measurements

Absorption spectra were recorded on a Varian Cary-100 spectrometer equipped with temperature control unit set at 298 K.

Results and discussion

Protonation

The stepwise protonation constants of **L** and $\mathbf{L^1}$ are reported in

Table 1 Stepwise protonation constants (log K) for receptors **L** and $\mathbf{L^1}$ determined in 0.15 mol dm^{-3} $NaClO_4$ at 298.1 ± 0.1 K

Reaction[a]	log K	
	L	$\mathbf{L^1}$
$H_{-1}\mathbf{L} + H \rightleftharpoons \mathbf{L}$[b]		11.30(5)
$\mathbf{L} + H \rightleftharpoons H\mathbf{L}$	9.30(3)[c]	10.08(3)
$H\mathbf{L} + H \rightleftharpoons H_2\mathbf{L}$	9.02(3)	9.52(4)
$H_2\mathbf{L} + H \rightleftharpoons H_3\mathbf{L}$	8.05(5)	8.28(4)
$H_3\mathbf{L} + H \rightleftharpoons H_4\mathbf{L}$	6.09(7)	6.05(5)
$H_4\mathbf{L} + H \rightleftharpoons H_5\mathbf{L}$	3.69(9)	4.01(5)
$H_5\mathbf{L} + H \rightleftharpoons H_6\mathbf{L}$	1.7(2)	2.11(7)

[a] Charges omitted for clarity. [b] $H_{-1}\mathbf{L}$ refers to the receptor in its fully deprotonated form including the OH group. [c] Numbers in parentheses are standard deviations in the last significant figure.

Table 1. The first aspect to be noted is that while **L** displays six protonation steps $\mathbf{L^1}$ has seven protonation steps, one of which should involve the phenolic group. **L** has relatively high constants for the three first protonation steps ($\log K_{HL} - \log K_{H_3L} = 2.25$), an intermediate one ($\log K_{H_3L} - \log K_{H_4L} = 1.96$) and much lower constants for the fifth and sixth protonation steps (($\log K_{H_4L} - \log K_{H_5L} = 2.4$). As has been extensively documented in the literature,[15–17] electrostatic considerations are the main factor explaining this grouping. As a matter of fact, while the binding of the first three protons to **L** can occur in nitrogen atoms distant enough not to cause high charge repulsion between same sign charges, the entrance of the fourth proton should take place next to an already protonated nitrogen atom, yielding therefore a greater decrease in basicity. Fifth and sixth protonations necessarily have to occur adjacent to two protonated nitrogens causing larger diminution of the protonation constants.

$H_{-1}\mathbf{L^1}$ presents a first constant much higher than the corresponding one of **L**, and also displays higher basicity than **L** in its second and third protonation steps (see Table 1) the constants for the next protonation steps of both ligands being much closer. A key point for understanding the acid–base behaviour of this receptor is to know at which stage the protonation of the phenolate group occurs. The NMR and UV-Vis spectra provide clear experimental evidence in this respect. Indeed, the ^{13}C NMR signal of the carbon nucleus labelled as B4 (see Chart 1) experiences a large upfield shift when passing from pH 8 (164 ppm) to pH 7 (156.9 ppm), $\Delta\delta = 7.1$ ppm corresponding with the fourth protonation step of $H_{-1}\mathbf{L^1}$, $H_3(H_{-1}\mathbf{L^1})^{2+} + H^+ \rightleftharpoons H_4(H_{-1}\mathbf{L^1})^{3+}$ [or $H_2(\mathbf{L^1})^{2+} + H^+ \rightleftharpoons H_3(\mathbf{L^1})^{3+}$], see distribution diagram in Fig. 1. The electronic absorption spectra recorded in aqueous solution at different pH values depicts clearly the involvement of the phenolic group in the protonation sequence. In fact, the wavelength of the absorbance maximum (λ_{max}/nm) and the molar absorptivity (ε/dm^3 mol^{-1} cm^{-1}) change from $\lambda_{max} = 277$ and $\varepsilon = 2360$ at pH = 2, where the species $H_6(\mathbf{L^1})^{6+}$ is prevalent in solution, to a spectrum showing two peaks at $\lambda_{max} = 242$ with $\varepsilon = 4100$ and $\lambda_{max} = 295$ with $\varepsilon = 4100$ at pH = 12 where the species $H_{-1}\mathbf{L^1}$ prevails. Such a change in λ_{max} is due to the presence of the phenolic form at low pH values and to the phenolate form at higher pH values. The passage from the phenolate to the phenol form starts at pH values around 8, corresponding to the presence of the $H_3(\mathbf{L^1})^{3+}$ species in solution (see Fig. 1). For example, in the $H_2(\mathbf{L^1})^{2+}$ there are three positive charges localized on the polyammonium centres and one negative on the phenolic oxygen. The high values of the first three protonation constants of $H_{-1}\mathbf{L^1}$ reported in Table 1 can find a plausible explanation in the formation of intramolecular hydrogen bonds between the protonated benzylic nitrogens and the deprotonated phenolate group at these stages.

Table 2 Cumulative and representative stability constants (log K) for the systems ADP–**L**, ATP–**L** and ATP–$\mathbf{L^1}$ determined at 298.1 K in 0.15 mol dm^{-3} $NaClO_4$

Reaction	log K		
	L		$\mathbf{L^1}$
	A ≡ ADP^{3-}	A ≡ ATP^{4-}	A ≡ ATP^{4-}
$A + H + \mathbf{L} \rightleftharpoons H\mathbf{L}A$[a]		12.90(2)	24.05(5)
$A + 2H + \mathbf{L} \rightleftharpoons H_2\mathbf{L}A$	22.00(2)	22.37(1)	33.49(4)
$A + 3H + \mathbf{L} \rightleftharpoons H_3\mathbf{L}A$	30.49(2)	31.00(2)	41.74(6)
$A + 4H + \mathbf{L} \rightleftharpoons H_4\mathbf{L}A$	37.96(2)	38.72(1)	49.50(2)
$A + 5H + \mathbf{L} \rightleftharpoons H_5\mathbf{L}A$	44.21(2)	45.31(2)	56.16(2)
$A + 6H + \mathbf{L} \rightleftharpoons H_6\mathbf{L}A$	49.16(2)	50.86(2)	61.52(2)
$A + 7H + \mathbf{L} \rightleftharpoons H_7\mathbf{L}A$	52.81(2)	54.90(2)	65.5(2)
$A + 8H + \mathbf{L} \rightleftharpoons H_8\mathbf{L}A$	55.05(6)	57.89(3)	68.15(3)
$A + H\mathbf{L} \rightleftharpoons H\mathbf{A}\mathbf{L}$		3.58	2.67
$A + H_2\mathbf{L} \rightleftharpoons H_2\mathbf{A}\mathbf{L}$	3.68	4.05	2.58
$A + H_3\mathbf{L} \rightleftharpoons H_3\mathbf{A}\mathbf{L}$	4.12	4.63	2.57
$A + H_4\mathbf{L} \rightleftharpoons H_4\mathbf{A}\mathbf{L}$	5.50	6.26	4.28
$HA + H_4\mathbf{L} \rightleftharpoons H_5\mathbf{A}\mathbf{L}$	5.59	6.61	4.77
$A + H_5\mathbf{L} \rightleftharpoons H_5\mathbf{A}\mathbf{L}$	8.06	9.16	6.99
$HA + H_5\mathbf{L} \rightleftharpoons H_6\mathbf{L}A$	6.85	8.48	6.13
$H_2A + H_4\mathbf{L} \rightleftharpoons H_6\mathbf{L}A$	6.64	8.16	6.13
$H_2A + H_5\mathbf{L} \rightleftharpoons H_7\mathbf{A}\mathbf{L}$	6.60	8.51	6.03
$HA + H_6\mathbf{L} \rightleftharpoons H_7\mathbf{A}\mathbf{L}$	8.79	10.81	10.04
$H_2A + H_6\mathbf{L} \rightleftharpoons H_8\mathbf{A}\mathbf{L}$	7.12	9.78	6.57

[a] Charges omitted for clarity. [b] Values in parentheses are standard deviations in the last significant figure.

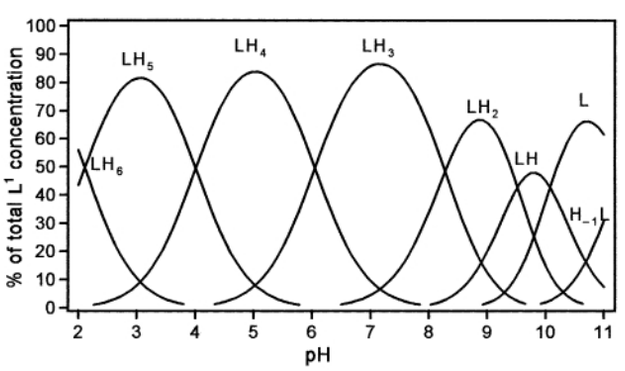

Fig. 1 Distribution diagrams of the system $\mathbf{L^1}$–H^+.

Interaction with the nucleotides and ATP cleavage

The stability constants for the formation of adduct species between ATP, ADP and **L** and ATP with $\mathbf{L^1}$ were determined by pH studies at 298.1 ± 0.1 K in 0.15 mol dm^{-3} $NaClO_4$ (Table 2). For the ATP systems the titration curves were carried out from alkaline to acidic pH in order to avoid hydrolysis of ATP in the course of the measurements. For this reason, the data below pH 3 were not considered in the models. In the pH range studied, adduct species with stoichiometries $AH_jL^{(j-n)+}$ ($j = 1$ to 8, A = ATP^{4-} and $j = 2$ to 8, A = ADP^{3-}) are formed. In the distribution diagrams shown in Fig. 2, it can be seen that while in the system ATP–**L** the adduct species prevail in solution below pH 9, in the system ATP–$\mathbf{L^1}$ the adduct species predominate only below pH 7, corresponding with the appearance in solution of the species $H_4(\mathbf{L^1})A^+$ or $H_5(H_{-1}\mathbf{L^1})A^+$. An analysis of the stability constants (Table 2) and of the selectivity profiles derived from the conditional stability constants[18–20] defined by eqn. (1)

$$K = \Sigma[AH_i + j\mathbf{L}]/\Sigma[H_iA]\Sigma[H_j\mathbf{L}] \quad (1)$$

shows that the interaction of **L** with ATP is much stronger than with ADP. Therefore, interaction of **L** with ATP is large enough to achieve quantitative complexation of ATP for stoichiometric **L**–ATP amounts and to induce selective recognition of ATP over ADP throughout a wide pH range (see Fig. 3).

Table 3 Rate constants (k/min^{-1}, estimated error ±6%) and activation parameters (kJ mol^{-1}) for the hydrolysis of ATP (0.01 mol dm^{-3}) or ADP (0.01 mol dm^{-3}) in the presence of **L** (0.01 mol dm^{-3})

Receptor	pH	T/°C	$k/10^{-3}$ min^{-1}	E_a[a]/kJ mol^{-1}	ΔH/kJ mol^{-1}	ΔG/kJ mol^{-1}	ΔS/J K^{-1} mol^{-1}
L(ATP)	3.0	35	30				
		40	46				
	5.2	35	14				
		40	23	72 ± 2	74 ± 2	97.5 ± 0.5	−75 ± 5
		50	43				
		55	80				
	5.7	40	12				
	7.5	40	1				
		70	29				
	9.0	70	3				
L(ADP)	3.0	70	40				
	4.0	50	4				
L^1(ATP)	4.2	40	19				
		50	44				
		60	122				
	5.0	60	19				
	6.4	50	2				
		70	5				

[a] Activation parameters calculated from $E_a = \Delta H + RT = -\mathrm{RTln}\,(kh/Tk_b)$ and $\Delta G = \Delta H - T\Delta S$, k_b = Boltzmann constant, h = Planck's constant and k the rate constant in s^{-1}.

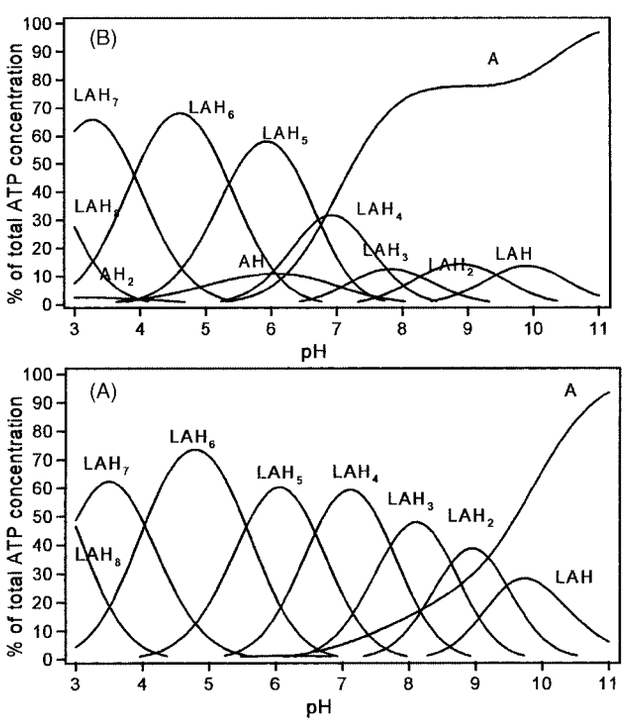

Fig. 2 Distribution diagrams for the systems: A) **L**–ATP–H$^+$ and B) **L**^{1}–ATP–H$^+$. [**L**] = [**L**^{1}] = [ATP] = 1 × 10^{-3} mol dm^{-3}.

Analogously, a comparison of the systems ATP–**L** and ATP–**L**^{1} shows that **L** interacts more strongly with ATP than **L**^{1} (see Figs. 2 and 3). It is also of interest to note the sudden decrease in the stability constants of the system ATP–**L**^{1} above pH 8 that accompanies the formation of the adduct $H_3A(\mathbf{L}^1)^{3+}$ [or $H_4A(H_{-1}\mathbf{L}^1)^{3+}$]. This diminution in stability can be explained by again taking into account the deprotonation of the phenolic group, which introduces a negative charge in the receptor and contributes unfavourably to the stability of the adduct species.

ATP Cleavage

At this point the first prerequisite for having an ATP catalyst, namely formation of relatively stable host–guest couples, has been fulfilled. However, it is well-known that the efficiency of a catalyst does not necessarily correlate with a very high stability of the adduct species and, very often, polyamines displaying large ATP affinities do not produce any rate enhancement of its hydrolysis (*vide infra*).

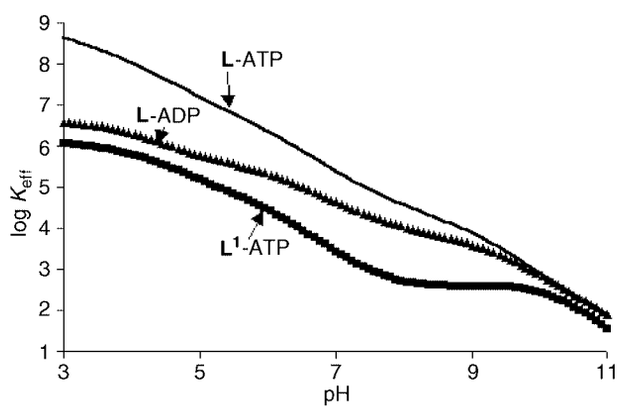

Fig. 3 Plot of the log of the conditional stability constants *vs.* pH for the system ATP–**L**, ADP–**L** and ATP–**L**^{1}.

The kinetic measurements of ATP hydrolysis were carried out by following the time-dependent change of the integrals from the resolved ^{31}P NMR signals of P_α, P_β and P_γ of ATP and peaks of inorganic phosphate. In the course of the reactions we did not observe signals attributable to pyrophosphate (Fig. 4). In the case of ADP hydrolysis P_α and P_β of ADP and inorganic phosphate were the signals followed. In Table 3 are included the rate constants obtained for the pseudo-first order hydrolysis of ATP at various pH values, along with some activation parameters. Comparison with the data from the literature is not straight forward due to the different concentrations and ionic strengths used. However, taking into account those differences, **L** presents rate enhancements which are, below pH 7, similar or even higher than those displayed by **O-bisdien** (for instance for [ATP] = [**O-bisdien**] = 3 × 10^{-3} mol dm^{-3} a value of k = 0.080 min^{-1} at 60 °C was reported in the pH range 2.5–7.5;[2] for [ATP] = [**O-bisdien**] = 0.01 mol dm^{-3}, ionic strength 0.3 mol dm^{-3} and pH = 3.6, values of k = 0.0037 min^{-1} and k = 0.029 min^{-1} were reported at T = 50 °C and 70 °C, respectively).[5]

The hydrolytic activity is strongly dependent on pH, decreasing as the pH is raised. Nevertheless, at pH 7.5 an important

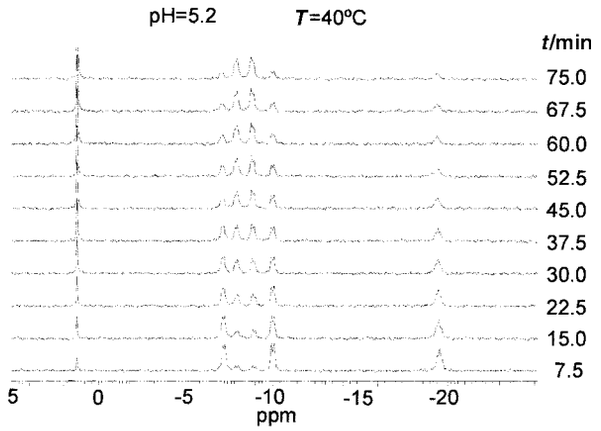

Fig. 4 Time evolution for ^{31}P NMR of solutions containing ATP and **L** in 1×10^{-2} mol dm^{-3} at 40 °C and pH = 5.2.

rate enhancement is still observed. It is also interesting to remark that the process is specific for the conversion of ATP into ADP, the subsequent transformation of ADP into AMP being much slower (see Table 3). The catalytic activity completely vanishes over pH 10, in agreement with the lack of formation of adducts at this pH value. The calculated activation parameters clearly show an unfavourable ΔS, which, as indicated by other authors, suggest an associative mechanism involving the addition of a nucleophile in the activation state that could also be a water molecule.[4,5] Attempts to identify a phosphoramidate intermediate have not been successful.[2,5]

Interestingly, the analogous metacyclophanes 2,5,8,11,14-pentaaza[15]metacyclophane (**L**^{2}) and 2,6,10,13,17,21-hexaaza[22]metacyclophane (**L**^{3}),[21,22] the first one displaying slightly smaller size and the second one larger size, do not increase at all the rate of ATP hydrolysis. Therefore, **L** falls within a well of maximum catalytic activity whose width is controlled by the molecular complementarity of host and guest species. **L** shares with [21]aneN_7 (see Chart 1) the same number of atoms forming the macrocyclic cavity and consequently should present a similar size.

Further support to the key role played by size complementarity in ATP activation is afforded by the study of the ATP–**L**^{1} system. Indeed, in Table 3 it can be seen that although not so high as in the ATP–**L** system, this system also displays relevant ATP rate enhancements from acidic pH to pH 7. At this pH the process slows down sharply, in concordance with the diminution of the stability of the adducts formed at this pH (*vide supra*). Indeed, deprotonation of the phenolic group of **L**^{1} would yield not only a destabilisation of the adduct species but also an important size reduction of the macrocyclic cavity. As suggested by molecular modelling this size reduction would be originated by intra-molecular hydrogen bonding between the protonated benzylic nitrogen atoms and the phenolate group. A combination of both these effects results in an almost complete quenching of the catalytic activity above pH 7 (see Table 3).

A final question concerns the role played by the aromatic ring in **L** in the recognition and in the catalytic events. ^1H NMR studies provide hints about the participation of π-stacking between adenine and the benzene spacer of **L** in the stabilisation of the anion complexes. The ^1H signals of the anomeric ATP protons (H1′, see Chart 1) are shifted upfield by 0.14 ppm and those of the adenine protons (H2 and H8) are also shifted upfield by 0.18 and 0.17 ppm, while those of the aromatic spacer, particularly HB2 and HB3, are shifted by 0.25 ppm, following the **L**–ATP interaction (Fig. 5). Interestingly, the protons of the ethylene chains of the polyamine bridges shift downfield *ca.* 0.2 ppm as a consequence of the interaction with the polyphosphate groups of the nucleotides. The benzylic protons (HB0) are shifted slightly upfield but the signal keeps its singlet characteristics. When a catalytic cycle is concluded and

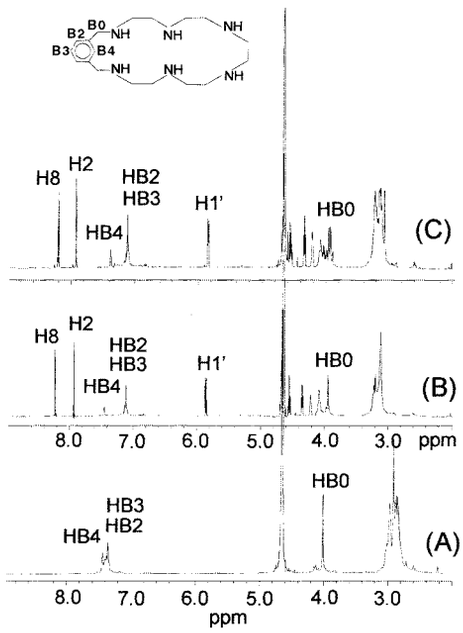

Fig. 5 ^1H NMR spectra of D_2O solutions at pD 7 of: A) **L**, B) **L** and ATP and C) **L** and ADP.

all ATP is converted into ADP, the ^1H signal of the benzylic protons is also shifted with respect to that of the free receptor at the same pH, but displays an AB spin system (Fig. 5C) denoting a freezing of the molecular movements at this side of the molecule.

Thus, it would seem that π-stacking contributes to stabilising the adduct **L**–ATP species and in rightly orienting the polyphosphate chain of ATP and the polyammonium bridge of the receptor for a good catalytic efficiency to be achieved.

Currently we are slightly modifying the structures of **L** and **L**^{1} in order to test the limits of the amplitude of the catalytic dimensional well. We also are investigating the influence of different metal ions in the process. We have also undertaken a molecular dynamics study to gain greater insight into the structural aspects governing these reactions.

Acknowledgements

We are indebted to DGICYT Project no. PB96-0792 and Generalitat Valenciana Project no. GV-D-CN-09-140 for financial support. Financial support by the Italian Ministero dell'Università e della Ricerca Scientifica e Tecnologica (COFIN98) is gratefully acknowledged.

References

1 J.-M. Lehn, *Angew. Chem., Int. Ed. Engl.*, 1988, **27**, 89; J.-M. Lehn, *Supramolecular Chemistry, Concepts and Perspectives*, VCH, Weinheim, 1995; *Supramolecular Chemistry of Anions*, eds. A. Bianchi, K. Bowman-James and E. García-España, Wiley-VCH, New York, 1997.

2 M. W. Hosseini, J.-M. Lehn and M. P. Mertes, *Helv. Chim. Acta*, 1983, **66**, 2454; M. W. Hosseini, A. J. Blacker and J.-M. Lehn, *J. Am. Chem. Soc.*, 1990, **112**, 3896; M. P. Mertes and K. B. Mertes, *Acc. Chem. Res.* 1990, **23**, 413.

3 A. Bencini, A. Bianchi, E. García-España, E. C. Scott, L. Morales, B. Wang, T. Deffo, F. Takusagawa, M. P. Mertes, K. Bowman Mertes and P. Paoletti, *Bioorg. Chem.*, 1992, **20**, 8; A. Andrés, C. Bazzicalupi, A. Bencini, A. Bianchi, V. Fusi, E. García-España, C. Giorgi, N. Nardi, P. Paoletti, J. A. Ramírez and B. Valtancoli, *J. Chem. Soc., Perkin Trans. 2*, 1994, 2367 and references therein.

4 A. Bencini, A. Bianchi, C. Giorgi, P. Paoletti, B. Valtancoli, V. Fusi, E. García-España, J. M. Llinares and J. A. Ramírez, *Inorg. Chem.*, 1996, **35**, 1114.

5 M. W. Hosseini, J.-M. Lehn, L. Maggiora, K. B. Mertes and M. P. Mertes, *J. Am. Chem. Soc.*, 1987, **109**, 537.

6 A. Bencini, M. I. Burguete, E. García-España, S. V. Luis, J. F. Miravet and C. Soriano, *J. Org. Chem.*, 1993, **58**, 4749.
7 E. García-España and S. V. Luis, *Supramol. Chem.*, 1996, **6**, 257.
8 A. Bencini, A. Bianchi, E. García-España, M. Micheloni and P. Paoletti, *Inorg. Chem.*, 1988, **27**, 176.
9 E. Bardazzi, M. Ciampolini, V. Fusi, M. Micheloni, N. Nardi, R. Pontellini and P. Romani, *J. Org. Chem.*, 1999, **64**, 1335.
10 E. García-España, M.-J. Ballester, F. Lloret, J.-M. Moratal, J. Faus and A. Bianchi, *J. Chem. Soc.*, *Dalton Trans.*, 1988, 101.
11 M. Fontanelli and M. Micheloni, *Proceedings of the 1st Spanish-Italian Congress on Thermodynamics of Metal Complexes*; Diputación de Castellón, Castellón, Spain, 1990.
12 G. Gran, *Analyst* (*London*), 1952, **77**, 881; F. J. Rossotti and H. Rossotti, *J. Chem. Educ.*, 1965, **42**, 375.
13 A. Sabatini, A. Vacca and P. Gans, *Coord. Chem. Rev.* 1992, **120**, 389; M. Micheloni, P. May and D. R. Williams, *J. Inorg. Nucl. Chem.*, 1978, **40**, 1209.
14 A. K. Convington, M. Paabo, R. A. Robinson and R. G. Bates, *Anal. Chem.*, 1968, **40**, 700.
15 A. Bencini, A. Bianchi, E. García-España, M. Micheloni and J. A. Ramírez, *Coord. Chem. Rev.*, 1999, **188**, 97.
16 J. Aragó, A. Bencini, A. Bianchi, E. García-España, M. Micheloni, J. A. Ramírez, P. Paoletti and P. Paoli, *Inorg. Chem.*, 1991, **30**, 1843; J. Aragó, A. Bencini, A. Bianchi, E. García-España, M. Micheloni, P. Paoletti, J. A. Ramírez and A. Rodríguez, *J. Chem. Soc.*, *Dalton Trans.*, 1991, 3077.
17 A. Bianchi, B. Escuder, E. García-España, S. V. Luis, V. Marcelino, J. F. Miravet and J. A. Ramírez, *J. Chem. Soc.*, *Perkin Trans. 2*, 1994, 1253.
18 A. Andrés, J. Aragó, A. Bencini, A. Bianchi, A. Doménech, V. Fusi, E. García-España, P. Paoletti and J. A. Ramírez, *Inorg. Chem.*, 1993, **32**, 3418; A. Bencini, A. Bianchi, M. I. Burguete, P. Dapporto, A. Doménech, E. García-España, S. V. Luis, P. Paoli and J. A. Ramírez, *J. Chem. Soc.*, *Perkin Trans. 2*, 1994, 569.
19 M. T. Albelda, M. A. Bernardo, E. García-España, M. L. Godino Salido, S. V. Luis, M. J. Melo, F. Pina and C. Soriano, *J. Chem. Soc.*, *Perkin Trans. 2*, 1999, 2545.
20 J. A. Aguilar, B. Celda, V. Fusi, E. García-España, S. V. Luis, M. C. Martínez, J. A. Ramírez, C. Soriano and R. Tejero, *J. Chem. Soc.*, *Perkin Trans. 2*, in the press (DOI: 10.1039/b000118j).
21 J. M. Llinares, PhD. Dissertation, Unversity of Valencia, 1997.
22 J. A. Aguilar, E. García-España, J. A. Guerrero, S. V. Luis, J. M. Llinares, J. A. Ramírez and C. Soriano, *J. Chem. Soc.*, *Chem. Commun.*, 1995, 2237; J. A. Aguilar, E. García-España, J. A. Guerrero, S. V. Luis, J. M. Llinares, J. A. Ramírez and C. Soriano, *Inorg. Chim. Acta*, 1996, **246**, 287.